

Empirically Analyzing Ethereum’s Gas Mechanism

Renlord Yang^{*§}, Toby Murray^{*}, Paul Rimba[§], Udaya Parampalli^{*}

^{*}School of Computing and Information Systems, University of Melbourne, Victoria, Australia

[§]Data61/CSIRO, Sydney, Australia

^{*}ryyang[at]student.unimelb.edu.au, toby.murray,udaya[at]unimelb.edu.au

[§]first.last[at]data61.csiro.au

Abstract—Ethereum’s Gas mechanism attempts to set transaction fees in accordance with the computational cost of transaction execution: a cost borne by default by every node on the network to ensure correct smart contract execution. Gas encourages users to author transactions that are efficient to execute and in so doing encourages node *diversity*, allowing modestly resourced nodes to join and contribute to the security of the network.

However, the effectiveness of this scheme relies on Gas costs being correctly aligned with observed computational costs in reality. In this work, we performed the first large scale empirical study to understand to what degree this alignment exists in practice, by collecting and analyzing Tera-bytes worth of nanosecond-precision transaction execution traces. Besides confirming potential denial-of-service vectors, our results also shed light on the role of I/O in transaction costs which remains poorly captured by the current Gas cost model. Finally, our results suggest that under the current Gas cost model, nodes with modest computational resources are disadvantaged compared to their better resourced peers, which we identify as an ongoing threat to node diversity and network decentralization.

I. INTRODUCTION

Cryptocurrency networks have seen massive growth and innovation, due to their decentralised nature and extensibility. The Ethereum network is a prime example, whose design aims to maximise extensibility while preserving decentralisation. Ethereum adopts Bitcoin’s proof-of-work distributed consensus mechanism and supports the execution of complex transactions through smart-contracts written in the Ethereum Virtual Machine (EVM) instruction set.

Given the gravity of decentralisation, *node diversity*—the ability for heterogeneous machines of varying capabilities to participate in the network—is a key consideration in the design of the EVM and setup of consensus parameters. In particular, Ethereum encourages anyone to freely join the network and participate even with modest computational resources without unduly hindering the network’s transaction throughput. Achieving decentralisation while maintaining diversity and throughput in an ecosystem of heterogeneous machines with differing computing capabilities is non-trivial because, by default, all network nodes are required to execute and check the results of each new transaction, to derive the current state of the network. Indeed, we argue that having a diversity of nodes able to check correct transaction execution is crucial for the network’s security, especially against the possibility of colluding miners.

To manage the cost of having nodes execute each new transaction, when a user creates a new transaction in Ethereum, the user must pay a fee for the network to execute the transaction. Part of this fee represents an approximation of the computational and storage cost of running the transaction. This fee is paid in virtual units, called Gas. The Gas mechanism therefore incentivises nodes to create transactions that are quick to execute as users optimise towards paying as little gas as possible. In addition, a block *gas limit* bounds the amount of gas that can be consumed by the transactions in any single block of Ethereum’s blockchain, approximating a per-block upper bound on the computational complexity of transaction execution and verification. In this way, Ethereum balances the freedom to create complex transactions against the need to ensure that transactions can be efficiently verified.

If gas is to maximally incentivise nodes to minimise variable computational costs, it is critical that it accurately reflects the real costs of transaction execution. To this end, the Ethereum Foundation has defined precise formulae for calculating gas costs for transactions, as a function of the transaction bytecode instructions [1]. Specifically, the current costs were defined by setting an ideal ratio R between execution time and units of gas on a single unidentified benchmark machine¹. By doing so each EVM instruction opcode was assigned a fixed gas cost that approximated its computational cost on the benchmark machine, calibrated relative to the other instructions.

The accuracy of this calibration directly influences the utility of Gas for incentivising transaction efficiency, and ensuring Ethereum can continue to maintain decentralization in the absence of trust in the face of increasing smart contract complexity. To evaluate the gas mechanism in its mission to price transactions effectively with respect to transaction execution time, we perform an in-depth empirical analysis of the Ethereum gas mechanics in an attempt to determine how they operate under real world usage scenarios. Our study was carried out by measuring transaction execution times across an interval of 2+ million blocks (post-EIP150) in the Ethereum blockchain, replaying all state transitions that have occurred since the genesis block. This allowed us to compute the observed Time-to-Gas ratio for each opcode, and their distributions, shedding light on the calibration precision of the

¹https://docs.google.com/spreadsheets/d/1n6mRqkBz3iWcOIRem_mO09GtSKEKrAsfO7Frgx18pNU/edit#gid=0

Gas mechanics. Our measurements were collected and contrasted between two machines: one highly efficient machine representing an upper bound on computational resources of individual Ethereum nodes and the other a typical desktop machine. Our contributions are as follows:

- A detailed collection of EVM traces for each transaction, with opcode execution times, measured on two disparate machines with defined specifications.
- We identify that some EVM opcodes are mispriced, particularly those involving disk I/O, presenting potential denial-of-service vectors.
- We analyse the effects of I/O and the impact of in-memory caching strategies employed by the reference client to mitigate I/O costs.
- We show that the current gas cost model favours more performant machines, which we identify as an ongoing threat to node diversity and decentralization.
- We briefly discuss possible solutions to these issues.

II. BACKGROUND

In this section, we will provide the building blocks for understanding how the Gas Mechanism operates in Ethereum.

A. Ethereum

The accounting unit for usage within the Ethereum network is known as Ether. Transactions in Ethereum utilise the *account* model of computation where each account is a reference to either a smart contract or a payment account. Both payment and smart contract accounts may send and receive Ethers.

The *Ethereum Virtual Machine* (EVM) is an interpreter which executes transactions that invoke smart contracts on the blockchain. Every participant in the Ethereum network operates an instance of the EVM and executes each new transaction. Doing so ensures that no node can lie about the results of a transaction undetected. The EVM implements the consensus rules that govern the validity of transactions, which includes the gas cost for each operator and other details (e.g., the block gas limit) that define valid state transitions.

The ordering of transactions is defined by their position in the blockchain and they are executed serially. Parallel verification of transactions [2] is non-trivial due to the possibility of side-effects via state mutation. As per other decentralised consensus network, Ethereum uses *Nakamoto Consensus* to order state transitions for its network state. Miners continuously solve proof-of-work puzzles to include valid transactions into blocks. All participants, miners and ordinary users alike verify every new transaction to independently derive the state of the network.

B. Transaction and State

Transactions describe state transitions in Ethereum. There are three types of transactions in Ethereum: transfer, message-call, and contract creation transactions. *Transfer* transactions transfer Ether balances from one account to another without the usage of the interpreter. *Message-call* transactions contain data payload which is used as an input to execute smart

contracts published on the Ethereum blockchain. *Contract creation* transactions publish new smart contracts onto the Ethereum blockchain. Accepting a transaction in Ethereum requires each participating node on the network to first verify the cryptographic seals and replaying the transaction. During the execution runtime for message-call transactions, gas is consumed for each executed EVM instruction.

Ethereum nodes across the network update their node state each time a new block is received. During the update process, nodes update various data structures stored locally which are used to verify future transactions, such as the state trie, account trie, transaction trie, and transaction receipts trie, which are all necessary to derive future block headers. The *state trie* is a record of the current state of all accounts and implemented as an authenticated data structure. Where possible, to mitigate I/O disk access, some elements of the state trie may be stored in memory for faster storage and retrieval to verify future transactions (see Section IV-B).

When joining the network, participating users have two ways to obtain the current state of the network. Firstly, they can bootstrap their nodes by performing *Initial Blocks Download* (IBD), aka a “full-sync”, to independently derive the current state of the network. During this process, the node must verify the cryptographic elements and replay all transactions for each block. Replaying transactions at the time of writing takes many weeks of serial computational time. Secondly, users can instead elect to obtain state snapshots from other peers (e.g., *fast-sync* [3] in *geth* and *warp-sync* in *parity*). Doing so allows the node to avoid having to replay all prior transactions. However, this comes at the price of having to trust in the honesty of a majority of its peers—a non-trivial trust assumption in the face of Sybil attacks [4].

C. Gas: Computation Virtual Unit

Gas [5], [1] is a virtual unit that is consumed when computation is performed by the EVM and exist to align computational cost to payable transaction fees. In effect, it discourages authored transactions which are computationally expensive to execute. When transactions are submitted to miners to be included in the blockchain, the author pays upfront a fixed amount of Gas. As part of the payment process, the author also bids for a gas price denominated in Ethers. The transaction fee for an authored transaction is a product of the amount of gas and the bid gas price.

For each computational step performed by the miner during verification, Gas is subtracted from the paid Gas. An Out-of-Gas exception is thrown by the EVM when Gas runs out. Such transactions are still included in the blockchain as proof that execution was attempted, and the gas paid is forfeited by the miner. On the other hand, valid transactions that have leftover gas will be refunded to transaction author.

D. Attacks

Attacks against decentralized cryptocurrency networks have been increasing over the past years due to its infancy and increased usage. On the networking layer, these networks are

susceptible to eclipse attacks, first explained by [6] prevents participants from consensus participation [7], [4]. On the EVM layer, numerous attacks [8] of varying severity exist. Notably, denial-of-service attacks mounted in the form of a resource exhaustion attack. Resource exhaustion attacks were first identified in [9] exploiting the fact that arbitrary inclusion of long-running transactions may be included by problem givers imposing an asymmetric amount of effort required to verify and execute these transaction to determine if the output is correct. Its impact when exploited with our observations in the EVM Gas Mechanism causes a significant reduction in transaction throughput and degradation in user experience as transactions take significantly longer to execute. Previously, between block 2.3M and 2.46M, a severe mispricing of gas cost for the `EXTCODESIZE` opcode [10] resulted in significantly longer transaction execution times across numerous blocks which resulted in the EIP150 hard-fork to introduce re-aligned gas cost for a number of EVM opcodes.

III. METHODOLOGY

As an attempt to evaluate the Gas Mechanism, we take time measurements on a per-opcode basis while transactions are executed by the EVM on two disparate machines. In this section, we describe the hardware, software, procedures and workloads undertaken to collect the measurements.

A. Hardware Specification

The first machine (A) used for experiment is a Dell R740xd and its setup is a dedicated server instance without any hypervisors nor guest VM instances. Table I lists the hardware specifications. While second machine (B), Dell Optiplex machine, representing a typical desktop node.

TABLE I
EXPERIMENTAL PLATFORMS

| Machine | A | B |
|----------------|-------------------------------------|------------------------------|
| Storage Type | PCIe NVMe SSD | SATA3 SSD |
| CPU | Intel® Xeon® Platinum 8180M@2.50GHz | Intel® Core™ i7-4770@3.40GHz |
| Threads (Core) | 2 (112) | 1 (4) |
| Cores (Socket) | 28 (56) | 4 (4) |
| Sockets | 2 | 1 |
| Memory | 1.5TB DDR4 2300MHz | 16GB DDR3 1600MHz |
| OS | Ubuntu 16.04 LTS | Ubuntu 16.04 LTS |
| Kernel | Linux 4.15.0-33 | Linux 4.15.0-33 |

These two different machines were chosen with the intent of allowing our results to extrapolated across the spectrum on typical Ethereum nodes at the time of writing. The key difference between our hardware choice and community-run Ethereum nodes is that most nodes are deployed in Virtual Private Server settings within data centres [11].

B. Software

The software implementation used is the C++ Ethereum reference implementation, also known as `aleth`² or `cpp-ethereum` previously. For compilation options, we compiled with default settings which uses LevelDB³ as the overlay DB back-end to manage the blockchain data and the state trie. We elected to use the C++ implementation as it is one of the reference implementations maintained by the Ethereum Foundation and it features relatively less runtime overhead compared to other implementations (*i.e.*, `geth`, `ethereumj`). Our methodology could be readily adapted to alternate software implementations, and doing so we leave as future work.

C. Setup

Our setup involve collecting nanosecond-precision transaction execution traces. Each transaction execution trace records the sequence of EVM opcodes (instructions) executed by the transaction and, for each element of the sequence, the length of time consumed by its execution in nanoseconds. Execution traces were output to a file through buffered I/O and then following the data collection were loaded into a database for further analysis. All data processing was performed outside of transaction execution to ensure that it did not directly interfere with our timing measurements. The logging of timing results was done using line buffered output stream. Intermittent buffer flushes occur outside of the runtime of EVM opcode instances guaranteeing the buffer flushes did not distort our time measurements. Our measurements exclude all time spent on other work such as the SHA3 computation for cryptographic transaction validation as we are only concerned with the performance of the EVM while executing transactions. We also omitted measurements for balance transfer transactions.

To collect our data, we forked the reference client⁴ to include the necessary code to perform timing measurements, making use of the standard `chrono` C++ library and user static tracing (UST) probing tool, `ltnng`.

The reference C++ client that we forked makes use of various in-memory software caches to avoid disk I/O. To understand their impact on transaction execution, we also added code to measure, for each transaction, the number of cache hits and misses. We logged cache hits and misses for in-memory caches

- Code Size Cache — caches code size of most recently used smart contract.
- Empty Account Cache — caches recently looked-up empty accounts.
- Account Cache — caches recently read account balances.
- Code Cache — caches recently used contract codes.

After the transaction traces were collected, we computed the the Time-to-Gas ratio for each opcode and performed statistical analysis for each opcode to visualise variability of the distribution which is shown in Table II and Table III.

²<https://github.com/ethereum/aleth>

³<http://leveldb.org/>

⁴at commit: `develop/aa73807c9a6f79114d36ce738658dcba0bc7fbb3`

IV. RESULTS

1) *Noise*: Any software measurement experiment is often subjected to noise due to the internal and competing processes in a system. We note that our experimental measurements cover a continuous data collection period that spans multiple weeks of real time. Our measurements cover transaction executions across 2 million blocks where the same set of EVM opcodes are repeatedly executed millions, if not billions of times. Therefore, we anticipate that measurement noise due to system resource contention will present as outliers in the data sets.

2) *System under test (SUT)*: Machine A is a dedicated server instance. During the data collection period, the Ethereum client was the only heavy workload process with metrics collected in a file for each transaction. Writes to the files were performed using buffered I/O with pre-allocated memory in the heap. The dedicated server instance is a multi-tenanted instance, therefore there are other processes that may have contended for IO access. However, we contend that the noise as a result of contention will be smoothed out with the high amount of collected traces. Machine B is a personal desktop machine. During the data collection period, the Ethereum client was run within a Linux control group with a RAM hard-cap limit of 8GB. Numerous other processes that contend with hardware resources were also running at the same time such as a web-browser, productivity tools, etc. We elected to use a noisy setup for Machine B as it is representative of the hardware choice used by a consumer user.

D. Workloads

We ran two types of workloads for the purpose of collecting EVM traces. From Section II, we noted that Ethereum opcodes require access to state which is stored on disk, therefore we also measured the time spent for low-level function calls to the client database interfaces.

First, the initial block download workload is used to gather measurements on all transactions since the genesis block up to block 4.7M. Between block 2.3M and 2.46M, a severe mispricing of gas cost for EVM opcodes that requires Disk I/O resulted in a denial of service attack. Discussed earlier in Section II-D, EIP150 [12] was implemented to permanently increase the cost of I/O-intensive opcodes to better align the verification time against gas cost. All transaction measurement data prior to EIP150 has been excluded from the results. This workload mimics a typical use scenario where transactions are continuously executed.

Second, we used `ltnng` [13] to collect more detailed traces of function calls in the database interface implemented by the client in an interval between two arbitrary block height. This technique enabled us to analyse internal function calls to the database interface and the time spent for each call to associated database interface functions. In contrast to other tracing tools, such as `Systemtap` and `uprobes` with `perf`, we found that instrumenting the client with `ltnng` traces enabled timing measurements with more precision.

In this section we present our measurements from the collected transaction traces of time and gas used during transaction execution.

A. Baseline

As mentioned in Section I the gas cost for each opcode was set in the consensus rule based on baseline measurements undertaken by the Ethereum foundation. The Ethereum foundation performed benchmarks to measure the approximate execution time of each opcode on an unidentified host machine. Then they set the gas cost for each opcode so that one unit of gas would represent approximately $1\mu s$ (1,000 nanoseconds) worth of computation, on that machine. Under this calibration, the baseline Time-to-Gas (aka Time/Gas) ratio of execution time in nanoseconds to gas used for each opcode is 1,000. Smaller values of this ratio represent better gas economy.

B. Observations

For each opcode we calculate its observed Time-to-Gas ratio for each of its executions in our recorded traces, by dividing its observed execution time by the amount of gas it is defined to consume under the current Gas cost model, mentioned above.

A total of 1TB worth of traces were collected on both SUTs and the ratios for each individual execution of each opcode was collected, and then grouped according to opcodes. Doing so allowed us to produce a full distribution of observed Time-to-Gas ratios for each opcode. Table II and Table III present a range of summary statistics that capture each distribution⁵.

The mean, μ is calculated by taking the average of the summation of all measured time-to-gas ratios. Q_1 and Q_3 respectively refer to the 25th and 75th percentile in data. The inter-quartile range (IQR) is calculated by taking the difference of $Q_3 - Q_1$. The Mean Absolute Deviation (MAD), a robust statistical method to compute variability in data [14], σ was computed using the method, $(\sum_{i=1}^n |x_i - Q_2|) \div n$. The Coefficient of Variability (CoV) [15], $\sigma \div \mu$ is used to measure the relative spread between different opcodes with respect to their individual distribution of observed ratios. Values in parentheses are computed by subtracting the mean/median against the baseline ratio of 1,000ns/gas and dividing by the original value, to measure how far the computed mean/median has deviated from the baseline. The number of observations for each opcode has also been included as a sanity check confirming that both machines executed the same exact transactions for our workload. † denotes opcodes that have high execution overhead due to the need to access the state trie. For the semantics of each EVM opcode, we refer the reader to the Ethereum yellowpaper [1].

Figure 1 is a diagram illustrating the measured execution time of the Trie DB lookup function used by state accessing EVM opcodes like `EXTCODESIZE` and `BALANCE`. The sampled interval is between 3,917,699 and 4,156,785

⁵More comprehensive results in a companion website is available at <https://github.com/renlord/bookish-octo-barnacle/blob/master/SNB2019.md>

TABLE II
SUMMARY STATISTICS FOR 10 SELECTED OPCODES BY THE HIGHEST MEAN RATIO ON MACHINE A AS DESCRIBED IN TABLE I.

| Opcode | Machine A | | | | | | | |
|--------------------------|-----------------|----------------|-------|----------|--------|---------------|--------------|-----------------------|
| | μ | Q_2 (Median) | Q_1 | Q_3 | IQR | #Observations | MAD σ | CoV $\sigma \div \mu$ |
| BLOCKHASH [†] | 34,343 (3,334%) | 110 (-89%) | 56.0 | 87,027.0 | 86,971 | 169,537 | 34,284.32 | 1.00 |
| SLOAD | 921 (-7%) | 32 (-96%) | 1.0 | 148.0 | 147 | 138,736,099 | 917.96 | 1.00 |
| BALANCE [†] | 867 (-13%) | 596 (-40%) | 509.0 | 692.0 | 183 | 8,644,400 | 400.32 | 0.46 |
| ORIGIN | 300 (-69%) | 289 (-71%) | 269.0 | 313.0 | 44 | 78,807 | 34.22 | 0.11 |
| ADDRESS | 297 (-70%) | 297 (-70%) | 262.0 | 318.0 | 56 | 5,123,311 | 38.67 | 0.13 |
| COINBASE | 286 (-71%) | 271 (-72%) | 250.0 | 312.0 | 62 | 58,315 | 38.73 | 0.13 |
| CALLER | 267 (-73%) | 261 (-73%) | 223.0 | 299.0 | 76 | 47,434,902 | 46.54 | 0.17 |
| MSTORE | 144 (-85%) | 134 (-86%) | 117.0 | 162.0 | 45 | 364,731,080 | 31.53 | 0.22 |
| CALLDATALOAD | 142 (-85%) | 134 (-86%) | 89.0 | 192.0 | 103 | 68,615,078 | 49.18 | 0.34 |
| EXTCODESIZE [†] | 142 (-85%) | 4 (-99%) | 2.0 | 27.0 | 25 | 12,386,619 | 141.00 | 0.99 |
| CODESIZE | 95 (-90%) | 53 (-94%) | 45.0 | 58.0 | 13 | 36,583 | 54.69 | 0.57 |
| SGT | 94 (-90%) | 58 (-94%) | 37.0 | 117.0 | 80 | 308,277 | 56.52 | 0.60 |
| MLOAD | 94 (-90%) | 76 (-92%) | 69.0 | 95.0 | 26 | 248,684,463 | 25.54 | 0.27 |
| DIV | 94 (-90%) | 89 (-91%) | 42.0 | 135.0 | 93 | 84,993,868 | 47.39 | 0.50 |
| SDIV | 85 (-91%) | 64 (-93%) | 38.0 | 106.0 | 68 | 162,142 | 48.00 | 0.56 |
| GASPRICE | 61 (-93%) | 48 (-95%) | 44.0 | 54.0 | 10 | 492,471 | 19.71 | 0.32 |
| PUSH5 | 56 (-94%) | 58 (-94%) | 41.0 | 65.0 | 24 | 355,623 | 13.91 | 0.24 |
| CALLDATASIZE | 50 (-94%) | 50 (-95%) | 42.0 | 55.0 | 13 | 26,912,010 | 10.12 | 0.20 |
| MULMOD | 48 (-95%) | 17 (-98%) | 12.0 | 80.0 | 68 | 3,279 | 36.29 | 0.75 |
| SLT | 46 (-95%) | 42 (-95%) | 37.0 | 49.0 | 12 | 4,399,360 | 10.36 | 0.22 |

TABLE III
SUMMARY STATISTICS FOR 10 SELECTED OPCODES BY THE HIGHEST MEAN RATIO ON MACHINE B AS DESCRIBED IN TABLE I.

| Opcode | Machine B | | | | | | | |
|--------------------------|-----------------|----------------|---------|----------|--------|---------------|--------------|-----------------------|
| | μ | Q_2 (Median) | Q_1 | Q_3 | IQR | #Observations | MAD σ | CoV $\sigma \div \mu$ |
| BLOCKHASH [†] | 35,156 (3,415%) | 117 (-88%) | 54.0 | 81,575.0 | 81,521 | 169,537 | 35,097.84 | 1.00 |
| SDIV | 26,854 (2,585%) | 85 (-91%) | 48.0 | 126.0 | 78 | 162,142 | 26,805.20 | 1.00 |
| SLOAD | 16,808 (1,580%) | 31 (-96%) | 0.0 | 201.0 | 201 | 138,736,099 | 16,805.73 | 1.00 |
| BALANCE [†] | 12,883 (1,188%) | 7,070 (607%) | 5,592.0 | 8,823.0 | 3,231 | 8,644,400 | 7,808.86 | 0.61 |
| SGT | 12,499 (1,149%) | 61 (-93%) | 45.0 | 136.0 | 91 | 308,277 | 12,454.36 | 1.00 |
| EXTCODESIZE [†] | 2,369 (136%) | 4 (-99%) | 2.0 | 26.0 | 24 | 12,386,619 | 2,367.62 | 1.00 |
| SLT | 1,459 (45%) | 85 (-91%) | 53.0 | 173.0 | 120 | 4,399,360 | 1,404.95 | 0.96 |
| DIV | 663 (-33%) | 120 (-88%) | 43.0 | 175.0 | 132 | 84,993,868 | 613.12 | 0.92 |
| ADDRESS | 351 (-64%) | 332 (-66%) | 304.0 | 381.0 | 77 | 5,123,311 | 53.26 | 0.15 |
| ORIGIN | 331 (-66%) | 316 (-68%) | 302.0 | 341.0 | 39 | 78,807 | 32.75 | 0.10 |
| CALLER | 328 (-67%) | 310 (-69%) | 263.0 | 355.0 | 92 | 47,434,902 | 60.05 | 0.18 |
| COINBASE | 326 (-67%) | 311 (-68%) | 300.0 | 331.0 | 31 | 58,315 | 28.33 | 0.09 |
| CALLDATALOAD | 237 (-76%) | 214 (-78%) | 172.0 | 269.0 | 97 | 68,615,078 | 60.82 | 0.26 |
| MLOAD | 179 (-82%) | 161 (-83%) | 157.0 | 184.0 | 27 | 248,684,463 | 22.57 | 0.13 |
| MULMOD | 176 (-82%) | 9 (-99%) | 9.0 | 55.5 | 46 | 3,279 | 167.45 | 0.95 |
| SSTORE | 144 (-85%) | 0 (-100%) | 0.0 | 0.0 | 0 | 42,213,319 | 144.87 | 1.00 |
| MSTORE | 143 (-85%) | 126 (-87%) | 113.0 | 159.0 | 46 | 364,731,080 | 38.45 | 0.27 |
| SUICIDE | 105 (-89%) | 0 (-100%) | 0.0 | 0.0 | 0 | 1,123 | 105.40 | 1.00 |
| AND | 102 (-89%) | 26 (-97%) | 19.0 | 40.0 | 21 | 285,047,447 | 83.26 | 0.81 |
| CALLDATASIZE | 100 (-89%) | 48 (-95%) | 41.0 | 102.0 | 61 | 26,912,010 | 61.58 | 0.61 |

[†] represents opcodes that belong in the `external` category which require read/write access to the state trie.

on Machine B (total 13,745,782 transactions). These time measurements were derived from traces were collected using code instrumented with the `ltnng` tracing framework. Due to limited privileges on Machine A and disk capacity limitations on Machine B, we could record these detailed traces only on Machine B and only for a limited workload. We discovered that the majority of time spent is focused on database operations associated with LevelDB instead of transaction execution. Duplication of EVM tracing show that the `ltnng` traces include approximately 100ns worth of overhead time.

V. DISCUSSION

From the results we infer three things. Firstly, certain opcode execution times have exceeded well beyond the baseline, which poses an attack vector for denial of service. Secondly, some opcodes have high variance in their ratio distributions further weakening the linear correlation between execution time and assigned gas cost. This poses an issue as an adversary can exploit this by authoring transactions that mimic the execution profile of high time-to-gas ratio transactions. Finally, our results also show that machines with different hardware capability yield different EVM execution profiles. We will

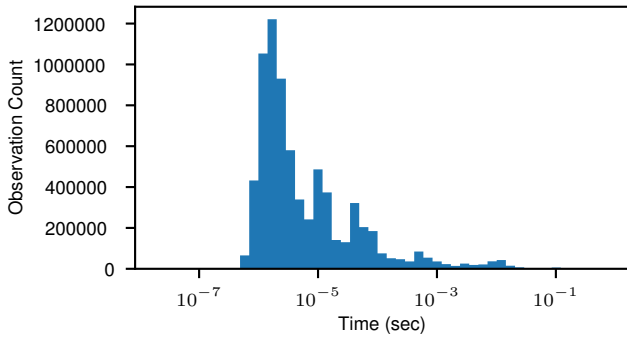


Fig. 1. Distribution of Trie DB lookup times when `EXTCODESIZE` or `BALANCE` was executed in the EVM. The sampled time measurements include both cache hit and miss lookups. The distribution of time measurements show variability in database lookup times with a median of 2.8us.

attempt to explain the cause of these observations in this section.

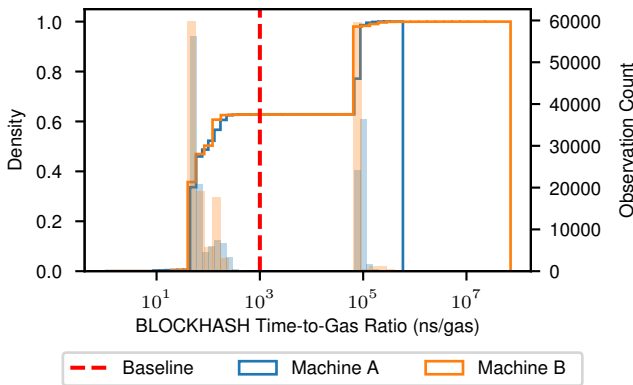


Fig. 2. Histogram plot (represented by shaded region) with CDF overlay (represented by solid lines) showing approximately 50% of `BLOCKHASH` execution instances performing worse than the baseline (denoted in dotted line along the vertical axis) posing a denial-of-service vulnerability on both machines. Overlapping regions indicate that the ratio distribution is identical across both machines.

a) *Denial-of-Service*: Underpriced gas cost for EVM opcodes pose a denial-of-service attack vector within the Ethereum ecosystem. While under the workload, both machines consistently shown that the `BLOCKHASH` opcode has the highest mean time-to-gas ratio well beyond the baseline which indicate that the opcode is severely underpriced and exploits can cause severe disruptions to all users.

The measured IQR further affirm that the opcode has been assigned with an incorrect gas cost as the ratio distribution is extremely sparse.

This opcode is one of the three opcode that falls under the `external` category as defined in the Ethereum yellowpaper as it requires access to the state trie during its execution. The main use of the opcode is to get the hash of one of the 256 most recent complete blocks. The main bottleneck for this particular opcode is caused by the fact that the `BLOCKHASH` EVM operation is implemented as a smart contract instead

of a built-in routine within the EVM. Therefore its execution requires traversing the state trie to load the contract code into RAM for execution. On top of that, in the reference implementation, there is also the overhead of creating an embedded EVM instance within the runtime of the base EVM executing the contract, incurring more overhead.

We note that this analysis applies only to the C++ reference implementation. Other users might, for instance, run custom, private implementations in which the `BLOCKHASH` opcode is implemented more efficiently, thereby avoiding this potential denial-of-service vector.

We note further that an impending change [16] to the gas cost for `BLOCKHASH` is scheduled to take place in the Constantinople hard-fork where the gas cost is raised from 20 to 800. Based on our results, this change would put its mean ratio below the baseline (1,000), which would fall from 35,000 to just 875.

b) *Gas Cost Misalignment*: Risk of denial of service aside, our measurements also show that on both experimental platforms, there are other EVM `external-class` opcodes (*i.e.*, `BALANCE`, `SLOAD` and etc) that have relatively higher variability in their time-to-gas ratio in comparison to other standard opcodes. While not directly a vulnerability, higher variability in ratio distribution make performance profiles unpredictable and opens up the possibility of transactions being executed at the expense of an unfairly high computational cost. This variability is generally caused by the fact that the client software must either load state trie objects from disk or a memory-resident cache. Due to the varying latencies posed by memory hierarchy in computing hardware, reading from a SSD disk can incur a 10 to 16 time penalty; on a HDD disk, this penalty could be 1,000 times larger. The nondeterminism of objects being resident in memory is the cause of the variability, which was further supported by our `ltnng` traces. The traces show that accessing a cached DB lookup is on average 100 times faster than it takes to process a DB lookup that requires disk access. From our measurements, we observed that on average, executing the `BALANCE` opcode requires 7 DB lookups, of which 1 or 2 will require disk access.

Most if not all Ethereum implementations use LevelDB as backend storage by default. LevelDB is a minimal key-value store database that provides an ordered mapping from string keys to string values. The associated overhead of looking up state during transaction execution is a consequence of how the state trie is stored internally within LevelDB. Recall that the state trie is an implementation of a Merkle Patricia Trie composed of three types of value nodes (*i.e.*, extension node, value node and index node). The traversal of the trie for any particular given value node has a theoretical constant lookup time which is the size of the query key. In the case of looking up an account balance, since Ethereum accounts are identified by keys of 20 bytes (40 hex characters) in length, the maximum number of traversal steps required will be 10. If there exist multiple value nodes that share common prefixes in their keys then this number of lookup steps can be reduced, by

utilising extension nodes (explained below). During a lookup the state root index is first retrieved, which resolves to an index node. The first element in the key is then used to retrieve subsequent index nodes or extension nodes. Extension nodes allow fast-track traversal along the state-trie reducing the need to traverse the full key length and can only be created when multiple node values share common substrings in their keys. Given the design of how state objects are retrieved, it is unsurprising to find that EVM opcodes that require state trie access exhibit high variability in their Time-to-Gas ratios.

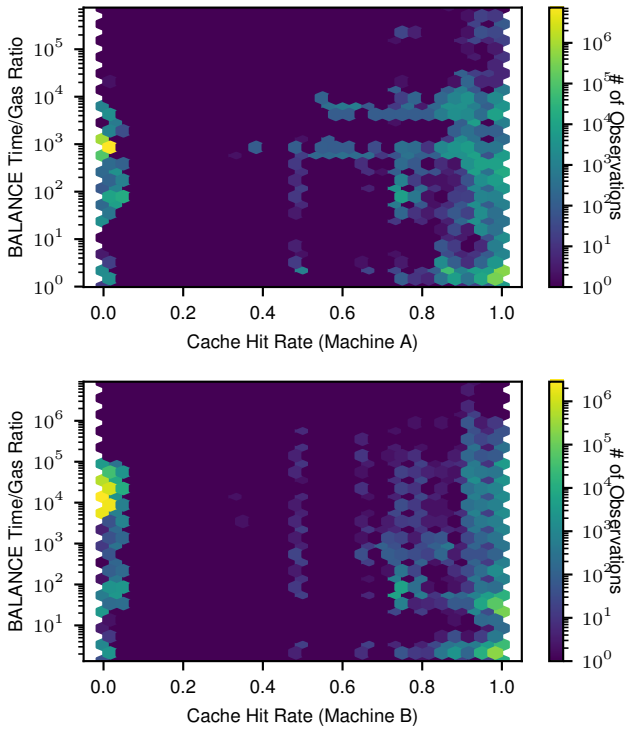


Fig. 3. Hexbin plot illustrating time to gas ratio versus account cache hit rate. This plot measures the effectiveness of maintaining an in-memory account cache. Lighter colored hexes indicate higher density of observation. The account cache is used by `BALANCE` and other opcodes that require loading an account into resident memory. Notice that with a 1.0 cache hit rate, the time/gas ratio demonstrates greater variance than with 0 cache hits highlighting cache inefficacy.

As a measure to smooth out this nondeterminism, `cpp-ethereum` implements a memory-resident cache which provides temporary caching of recently accessed state objects (*e.g.*, accounts, code sizes, etc) as discussed earlier in Section II. Not to be confused with the LRU Cache used by LevelDB, the caching policy for these memory-resident caches is determined by the Ethereum client; whereas what gets stored in the LevelDB cache is not controlled by the client. Due to frequent state changes following each block, the custom implemented account cache is invalidated when state is finalised. To study the effectiveness of the memory-resident cache implementation, we measured the account cache hit rate which tracks the percentage of cache hits when the

EVM runtime attempts to lookup an account in the state trie. It is used for all opcodes that require an account lookup such as `BALANCE`. Our measurements in Figure 3 show that the account cache is mildly effective at improving the Time-to-Gas ratio. On machine B, the advantages of having the account cache appears marginal.

Cache efficiency is typically realised when programs have strong locality of reference. We observed that during the runtime of smart contracts in our workload, usage of the `BALANCE` opcode often referenced different account balances which resulted in poor spatial locality. On the other hand, we observe that the use of caching for `EXTCODESIZE` to be more effective: the majority of the ratio distribution is below the baseline (1,000 ns/gas), with a mean that is below 100 ns/gas. We attribute this improvement to two usage traits. Firstly, the `EXTCODESIZE` opcode is often used to check code sizes of well-known address locations. Secondly, the code size for an address is unlikely to change once code has been authored for that address: Ethereum smart contracts are immutable until the `SUICIDE` opcode is called (which deletes them). In contrast, account balances change often, which causes cached values in the account cache to be frequently invalidated reducing cache effectiveness. Therefore, we emphasize that memory-resident caching appears to be sub-optimally effective to improve EVM execution performance for opcodes that require account lookups.

c) Hardware Choices: Choice of hardware when running an Ethereum node plays a significant factor for performance and the efficacy of keeping up with consensus. We observed that despite running with competent consumer hardware machines (*i.e.*, Machine B), it is still possible for the node to lag behind consensus as more capable machines (likely to be used by miners) can outperform less capable machines. Significant mean and σ (mean absolute deviation) differences for identical opcodes on the two machines were observed. Generally, both mean and mean absolute deviation observed on Machine B are higher than observed on Machine A. This deviation highlights that machines with better hardware specifications are likely to outperform lesser capable machines. This is especially problematic as miners are usually well-resourced, running nodes on powerful machines. Such miners will have relatively better gas economy while executing EVM transaction in contrast to *e.g.*, machines used in domestic households.

We argue that this competitive advantage in gas economy for the well-resourced poses a threat to node diversity and decentralisation. Specifically, it indicates that mining nodes with better hardware will gain a competitive edge while extending the canonical chain, while nodes running on lesser hardware will instead contribute to higher fork occurrences. Nodes with similar specifications to Machine B are less likely to keep up with consensus, especially if (as indicated in Figure 5) gas economy deteriorates over time due to increased read amplification. In light of this, we suggest that consensus networks consider recommending minimal hardware requirements for effective participation in consensus.

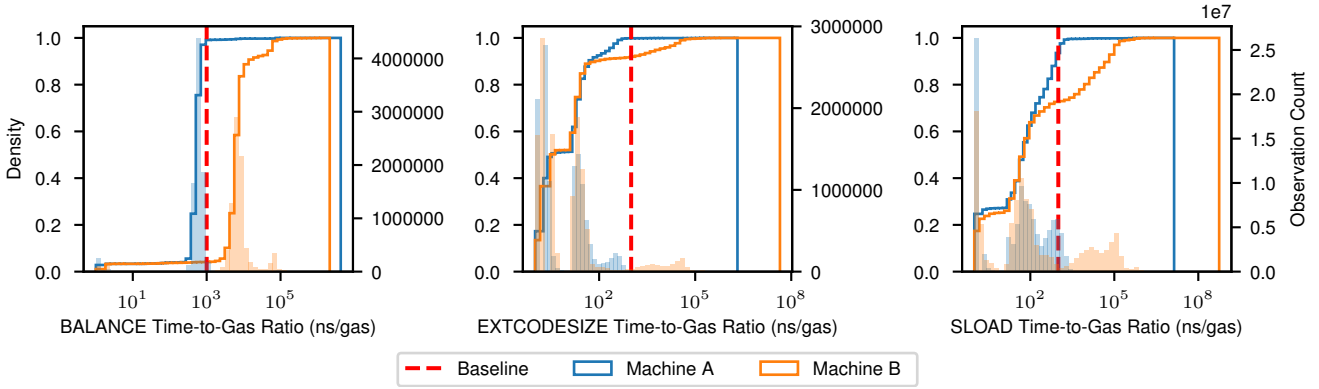


Fig. 4. Distribution of BALANCE, EXTCODESIZE and SLOAD time-to-gas ratios showing that Machine B contains execution instances of the BALANCE opcode running longer than execution instances on Machine A by a factor of 10 to 100. Increasing time-to-gas ratio represents increasing unit time spent per unit gas. The degree of misalignment is measured by the amount of ratios observed above (to the right of) the baseline. Hardware choice effects are measured by the union of overlapping distribution of ratio values. Evidently, hardware choice plays a significant factor in the runtime of BALANCE and also causes a misalignment in its gas cost. Some minor misalignment as a consequence of hardware choice is also observed for both EXTCODESIZE and SLOAD for Machine B.

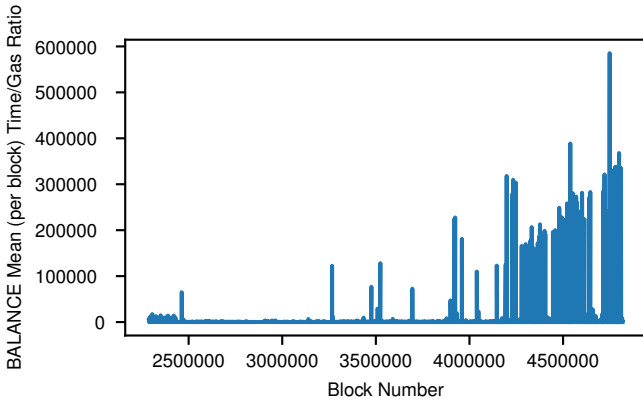


Fig. 5. Plot showing deterioration of BALANCE opcode as block number increases. As the state size grows, external opcodes efficiency deteriorate due to increased read amplification when accessing data values from disk.

Significant deviation in performance due to hardware is particularly observable for the BALANCE opcode, whose distribution of observed Time-to-Gas ratios varies greatly between Machine A and Machine B (see Figure 4). The difference is so large that in the event that both machines were operated by miners, we contend that Machine B is almost guaranteed to lose out in the race for consensus. The difference between the two machines in terms of their ratio distribution further confirms that hardware capability is a key factor in the gas economy of a node. Furthermore, we also observed that Machine A and B have distinct runtime profiles. Nearly all BALANCE opcode executions run below the baseline ratio for Machine A, while only 10% of BALANCE executions run below the baseline for Machine B.

As a general observation, we observed that time-to-gas ratios on Machine B are generally higher than Machine A and this difference is more profound for external class

opcodes. Other opcodes show negligible difference and still run below the baseline. This difference further confirms that hardware choice does play a significant role in an operator’s efficiency and tendency to keep up to consensus.

Aside from the mean ratio differences between the two machine, we also observe that on average the assigned gas cost for non-external opcodes are higher than external opcodes. Therefore, it appears as if users have been paying relatively more in Gas for computational opcodes compared to external opcodes.

The observed variation in ratio distributions between the two machines indicates that the Gas cost model is ineffective for maintaining fairness between nodes running different hardware. We argue that, due to this variation, the Ethereum ecosystem will tend to centralization as lesser hardware has relatively fewer incentives to race for consensus. The reduced incentives for lesser nodes to participate increases the barriers to entry for consensus participation and, we argue, so threatens node diversity. It also reduces the potential for network decentralization, since lesser capable nodes must either give up on verifying future transaction executions or fall out of consensus.

VI. POSSIBLE SOLUTIONS

In the previous section, we identified key problems that led to highly volatile time-to-gas ratio distributions for various EVM opcodes. These key problems are mainly exacerbated by the dependency of transaction execution on state. As a direct measure to reduce this variance in ratio distribution, we can either reduce state access during transaction runtime or improve I/O performance and predictability when state is being accessed. In this section, we outline existing research and potential implementation avenues that can be applied to address this problem.

One way improve I/O performance when reading state data is to optimize the database backend used to store

and read state data. Volatile database lookup times suffer from read-amplification introduced by LevelDB storage. Read-amplification occurs when the number of read operations executed by the database driver exceeds a single query against the disk. [?] proposes a novel database implementation to store the Ethereum state objects which improves read and write performance by reducing read and write amplification.

Longer term solutions that aim to curb the state growth on a single node include blockchain sharding and state channels. State channels enable the aggregation of transaction executions that persist all interim state changes in a single transaction on the blockchain. Proposed state channel solutions are similar to micro-payment channel schemes proposed in Bitcoin such as [17], [18] but envisioned to be more generic to allow for more general purpose computation to take place between two private parties. Blockchain sharding solutions such as [19], [20], [21], [22] aim to split the network into shards (*i.e.*, subset of nodes) that are responsible for a subset of the full state. While not directly addressing the key problems discussed in the previous section, proposed sharding scheme can alleviate the problem by curbing node state growth. Sharding schemes introduce additional security assumptions that enable nodes to process state changes that they cannot independently verify.

Finally, verifiable computing methods [23], [?] have also been proposed as a potential solution to avoid the need for transaction execution. Such schemes allow a node to verify that a transaction has been correctly executed without having to re-execute the transaction to independently derive its result, using embedded zero-knowledge proofs. These proofs can be checked in time independent of the size of the transaction. Yet at the time of writing have yet to be deployed.

VII. RELATED WORKS

Our work is closely related to [?], which briefly measured the performance of a handful of Ethereum opcodes, and compared the results between two similar machines running different operating systems. None of the opcodes considered in their analysis access the state trie (*i.e.*, perform I/O), and their measurements cover synthetic benchmarks only for a relatively small number of executions. Thus, unlike our results, theirs do not easily generalise to real-world usage nor shed light on the impact of I/O on the current Gas cost model, which we found to be a major source of misalignment. Finally, their results shed little light on the plight of modest nodes vs their more computationally resourced peers, which we identify as a threat to node diversity.

Empirical measurements have provided us with a better understanding of decentralized cryptocurrency networks. [24] measured block and transaction propagation delays in Bitcoin and produced a model which led to future security studies and the discovery of numerous attacks such as [25], [26], [27]. [?] measured decentralized metrics in both Bitcoin and Ethereum networks such as the distribution of hash power held by miners and the distribution of network peers by geography, to quantitatively understand the degree of decentralization. [28], [11] extend our understanding of the Ethereum network

by adding measurements of client heterogeneity, connectivity between peers and geographical distribution of peers. Other measurement and tracing work such as [29], [30], [31] involve the analysis of the security of the underlying network which led to a better understanding of the decentralized network security model. [32] is a community-run Ethereum block explorer which also collects EVM traces for each transaction. Our work extends these traces by also including measured time for each EVM operation, and carefully analysing the effectiveness of the current Gas cost model.

Other works have focused on smart contract use, [33] quantified the number of smart contracts in application domains for usage pattern analysis in Bitcoin and Ethereum. [34] extend this by analyzing behavioral usage patterns by network users and clustering contracts based on code similarity.

Efforts to improve verification throughput have prompted a flurry of studies in speculative concurrent execution of EVM transactions. [35], [2] proposed adding concurrency in smart contracts and showed that it was possible to execute smart contracts concurrently by analysing transaction dependencies to run non-conflicting transactions in parallel. Subsequently, [36] introduced the first framework for optimistic concurrent execution of smart contracts which leverages basic/multi-version timestamp ordering. Finally, [37] carried out a measurement study on simulated greedy concurrent transaction execution. Our measurements and analysis assume serial transaction execution, as implemented in the main Ethereum clients; however extending them to concurrent execution could be an interesting avenue for future research.

VIII. CONCLUSION

To the best of our knowledge, we performed the first large scale empirical analysis of the EVM Gas mechanism and the current Gas cost model. We confirmed potential denial-of-service vectors resulting from mis-priced EVM opcodes involving disk I/O. We also measured the effects of I/O in transaction costs, finding that it remains poorly captured by the current Gas cost model and that its effects are getting worse over time. We also found that under the current Gas cost model, nodes with modest computational resources are disadvantaged compared to their better resourced peers, which we identified as an ongoing threat to node diversity and network decentralization. Our results indicate that, absent deployment of techniques such as verifiable computation that allow transactions to be verified without re-executing them, further work is required to improve Ethereum's Gas cost model to better align Gas costs with transaction execution costs.

REFERENCES

- [1] G. Wood, "Ethereum: A secure decentralised generalised transaction ledger."
- [2] L. Yu, W.-T. Tsai, G. Li, Y. Yao, C. Hu, and E. Deng, "Smart-contract execution with concurrent block building," in *2017 IEEE Symposium on Service-Oriented System Engineering (SOSE)*, IEEE, Apr. 2017, pp. 160–167. [Online]. Available: <https://doi.org/10.1109/sose.2017.33>
- [3] P. Szilgyi, "Github PR: Eth/63 fast synchronization algorithm," <https://github.com/ethereum/go-ethereum/pull/1889>, 2015, [Online; accessed 20-May-2018].

- [4] Y. Marcus, E. Heilman, and S. Goldberg, "Low-resource eclipse attacks on ethereum's peer-to-peer network," *IACR Cryptology ePrint Archive*, vol. 2018, p. 236, 2018. [Online]. Available: <http://eprint.iacr.org/2018/236>
- [5] Ethereum Contributors, "Ethereum whitepaper," <https://github.com/ethereum/wiki/wiki/White-Paper>, 2014, [Online; accessed 20-May-2018].
- [6] A. Singh, T.-W. Ngan, P. Druschel, and D. S. Wallach, "Eclipse attacks on overlay networks: Threats and defenses," in *Proceedings IEEE INFOCOM 2006. 25TH IEEE International Conference on Computer Communications*. IEEE, 2006. [Online]. Available: <https://doi.org/10.1109/infocom.2006.231>
- [7] E. Heilman, A. Kendler, A. Zohar, and S. Goldberg, "Eclipse attacks on bitcoin's peer-to-peer network," in *24th USENIX Security Symposium, USENIX Security 15, Washington, D.C., USA, August 12-14, 2015.*, 2015, pp. 129–144. [Online]. Available: <https://www.usenix.org/conference/usenixsecurity15/technical-sessions/presentation/heilman>
- [8] N. Atzei, M. Bartoletti, and T. Cimoli, "A survey of attacks on ethereum smart contracts (sok)," in *Principles of Security and Trust - 6th International Conference, POST 2017, Held as Part of the European Joint Conferences on Theory and Practice of Software, ETAPS 2017, Uppsala, Sweden, April 22-29, 2017, Proceedings*, 2017, pp. 164–186. [Online]. Available: https://doi.org/10.1007/978-3-662-54455-6_8
- [9] L. Luu, J. Teutsch, R. Kulkarni, and P. Saxena, "Demystifying incentives in the consensus computer," in *Proceedings of the 22nd ACM SIGSAC Conference on Computer and Communications Security - CCS '15*, ACM. ACM Press, 2015, pp. 706–719. [Online]. Available: <https://doi.org/10.1145/2810103.2813659>
- [10] Ethereum Foundation, "The Ethereum network is currently undergoing a DoS attack," <https://blog.ethereum.org/2016/09/22/ethereum-network-currently-undergoing-dos-attack/>, 2016.
- [11] S. K. Kim, Z. Ma, S. Murali, J. Mason, A. Miller, and M. Bailey, "Measuring Ethereum network peers," in *Proceedings of the Internet Measurement Conference 2018*, ser. IMC '18. New York, NY, USA: ACM, 2018, pp. 91–104. [Online]. Available: <http://doi.acm.org/10.1145/3278532.3278542>
- [12] V. Buterin, "EIP150: Gas cost changes for IO-heavy operations," <https://github.com/ethereum/EIPs/blob/master/EIPS/eip-150.md>, 2016, [Online; accessed 20-May-2018].
- [13] M. Desnoyers and M. R. Dagenais, "The LTTng tracer: A low impact performance and behavior monitor for gnu/linux," in *OLS (Ottawa Linux Symposium)*, vol. 2006, 2006, pp. 209–224.
- [14] P. J. Huber, *Robust Statistics*. John Wiley & Sons, Inc., Feb. 1981. [Online]. Available: <https://doi.org/10.1002/0471725250>
- [15] H. Abdi, "Coefficient of variation," *Encyclopedia of research design*, vol. 1, pp. 169–171, 2010.
- [16] "Fix BLOCKHASH cost in Constantinople," <https://github.com/ethereum/aleth/pull/5314>, accessed: 2018-08-30.
- [17] C. Decker and R. Wattenhofer, "A fast and scalable payment network with bitcoin duplex micropayment channels," in *Lecture Notes in Computer Science*. Springer International Publishing, 2015, pp. 3–18. [Online]. Available: https://doi.org/10.1007/978-3-319-21741-3_1
- [18] J. Poon and T. Dryja, "The Bitcoin Lightning network: Scalable off-chain instant payments," Technical Report (draft). <https://lightning.network>, Tech. Rep., 2015.
- [19] M. Al-Bassam, A. Sonnino, S. Bano, D. Hryczyszyn, and G. Danezis, "Chainspace: A sharded smart contracts platform," in *Proceedings 2018 Network and Distributed System Security Symposium*. Internet Society, 2018. [Online]. Available: <https://doi.org/10.14722/ndss.2018.23241>
- [20] E. Kokoris-Kogias, P. Jovanovic, L. Gasser, N. Gailly, E. Syta, and B. Ford, "OmniLedger: A secure, scale-out, decentralized ledger via sharding," in *2018 IEEE Symposium on Security and Privacy (SP)*, IEEE. IEEE, May 2018, pp. 583–598. [Online]. Available: <https://doi.org/10.1109/sp.2018.000-5>
- [21] L. Luu, V. Narayanan, C. Zheng, K. Baweja, S. Gilbert, and P. Saxena, "A secure sharding protocol for open blockchains," in *Proceedings of the 2016 ACM SIGSAC Conference on Computer and Communications Security - CCS'16*, ACM. ACM Press, 2016, pp. 17–30. [Online]. Available: <https://doi.org/10.1145/2976749.2978389>
- [22] D. Sel, K. Zhang, and H.-A. Jacobsen, "Towards solving the data availability problem for sharded ethereum," in *Proceedings of the 2nd Workshop on Scalable and Resilient Infrastructures for Distributed Ledgers - SERIAL'18*, ACM. ACM Press, 2018, pp. 25–30. [Online]. Available: <https://doi.org/10.1145/3284764.3284769>
- [23] E. Ben-Sasson, A. Chiesa, D. Genkin, E. Tromer, and M. Virza, "Snarks for C: verifying program executions succinctly and in zero knowledge," in *Advances in Cryptology - CRYPTO 2013 - 33rd Annual Cryptology Conference, Santa Barbara, CA, USA, August 18-22, 2013. Proceedings, Part II*, 2013, pp. 90–108. [Online]. Available: https://doi.org/10.1007/978-3-642-40084-1_6
- [24] C. Decker and R. Wattenhofer, "Information propagation in the bitcoin network," in *IEEE P2P 2013 Proceedings*, IEEE. IEEE, Sep. 2013, pp. 1–10. [Online]. Available: <https://doi.org/10.1109/p2p.2013.6688704>
- [25] I. Eyal and E. G. Sirer, "Majority is not enough," *Commun. ACM*, vol. 61, no. 7, pp. 95–102, Jun. 2018. [Online]. Available: <https://doi.org/10.1145/3212998>
- [26] K. Nayak, S. Kumar, A. Miller, and E. Shi, "Stubborn mining: Generalizing selfish mining and combining with an eclipse attack," in *2016 IEEE European Symposium on Security and Privacy (EuroS&P)*, IEEE. IEEE, Mar. 2016, pp. 305–320. [Online]. Available: <https://doi.org/10.1109/eurosp.2016.32>
- [27] A. Sapirshstein, Y. Sompolinsky, and A. Zohar, "Optimal selfish mining strategies in bitcoin," in *Financial Cryptography and Data Security - 20th International Conference, FC 2016, Christ Church, Barbados, February 22-26, 2016, Revised Selected Papers*, 2016, pp. 515–532. [Online]. Available: https://doi.org/10.1007/978-3-662-54970-4_30
- [28] L. Anderson, R. Holz, A. Ponomarev, P. Rimba, and I. Weber, "New kids on the block: An analysis of modern blockchains," *arXiv e-prints*, p. arXiv:1606.06530, Jun. 2016.
- [29] M. Fleder, M. S. Kester, and S. Pillai, "Bitcoin transaction graph analysis," *CoRR*, vol. abs/1502.01657, 2015. [Online]. Available: <http://arxiv.org/abs/1502.01657>
- [30] P. Koshy, D. Koshy, and P. D. McDaniel, "An analysis of anonymity in bitcoin using P2P network traffic," in *Financial Cryptography and Data Security - 18th International Conference, FC 2014, Christ Church, Barbados, March 3-7, 2014, Revised Selected Papers*, 2014, pp. 469–485. [Online]. Available: https://doi.org/10.1007/978-3-662-45472-5_30
- [31] D. Ron and A. Shamir, "Quantitative analysis of the full bitcoin transaction graph," in *Financial Cryptography and Data Security - 17th International Conference, FC 2013, Okinawa, Japan, April 1-5, 2013, Revised Selected Papers*, 2013, pp. 6–24. [Online]. Available: https://doi.org/10.1007/978-3-642-39884-1_2
- [32] Etherscan Developers, "Etherscan," 2018, <https://etherscan.io>.
- [33] M. Bartoletti and L. Pompianu, "An empirical analysis of smart contracts: Platforms, applications, and design patterns," in *Financial Cryptography and Data Security - FC 2017 International Workshops, WAHC, BITCOIN, VOTING, WTSC, and TA, Sliema, Malta, April 7, 2017, Revised Selected Papers*, 2017, pp. 494–509. [Online]. Available: https://doi.org/10.1007/978-3-319-70278-0_31
- [34] L. Kiffer, D. Levin, and A. Mislove, "Stick a fork in it," in *Proceedings of the 16th ACM Workshop on Hot Topics in Networks - HotNets-XVI*, ser. IMC '18. New York, NY, USA: ACM Press, 2017, pp. 494–499. [Online]. Available: <https://doi.org/10.1145/3152434.3152449>
- [35] T. Dickerson, P. Gazzillo, M. Herlihy, and E. Koskinen, "Adding concurrency to smart contracts," in *Proceedings of the ACM Symposium on Principles of Distributed Computing - PODC '17*, ACM. ACM Press, 2017, pp. 303–312. [Online]. Available: <https://doi.org/10.1145/3087801.3087835>
- [36] P. Singh Anjana, S. Kumari, S. Peri, S. Rathor, and A. Somani, "An Efficient Framework for Optimistic Concurrent Execution of Smart Contracts," *arXiv e-prints*, p. arXiv:1809.01326, Sep. 2018.
- [37] V. Saraph and M. Herlihy, "An Empirical Study of Speculative Concurrency in Ethereum Smart Contracts," *arXiv e-prints*, p. arXiv:1901.01376, Jan. 2019.